

# A SUPER-EDDINGTON WIND SCENARIO FOR THE PROGENITORS OF TYPE Ia SUPERNOVAE

Xin Ma<sup>1,2,3</sup>, Xuefei Chen<sup>1,2</sup>, Hai-liang Chen<sup>1,2,3</sup>, Pavel A. Denissenkov<sup>4,5</sup>, Zhanwen Han<sup>1,2</sup>

## ABSTRACT

The accretion of hydrogen-rich material onto carbon-oxygen white dwarfs (CO WDs) is crucial for understanding type Ia supernova (SN Ia) from the single-degenerate model, but this process has not been well understood due to the numerical difficulties in treating H and He flashes during the accretion. For the CO WD masses from 0.5 to 1.378  $M_{\odot}$  and accretion rates in the range from  $10^{-8}$  to  $10^{-5} M_{\odot} \text{ yr}^{-1}$ , we simulated the accretion of solar-composition material onto CO WDs using the state-of-the-art stellar evolution code of MESA. For comparison with the steady-state models (e.g Nomoto et al. (2007)), we firstly ignored the contribution from nuclear burning to the luminosity when determining the Eddington accretion rate and found that the properties of H burning in our accreting CO WD models are similar to those from the steady-state models, except that the critical accretion rates at which the WDs turn into red giants or H-shell flashes occur on their surfaces are slightly higher than those from the steady-state models. However, the super-Eddington wind is triggered at much lower accretion rates, than previously thought, when the contribution of nuclear burning to the total luminosity is included. This super-Eddington wind naturally prevents the CO WDs with high accretion rates from becoming red giants, thus presenting an alternative to the optically thick wind proposed by Hachisu et al. (1996). Furthermore, the super-Eddington wind works in low-metallicity environments, which may explain SNe Ia observed at high redshifts.

---

<sup>1</sup>Yunnan Observatories, Chinese Academy of Sciences, Kunming 650011, China, maxin@ynao.ac.cn, cxf@ynao.ac.cn

<sup>2</sup>Key Laboratory for the Structure and Evolution of Celestial Objects, Chinese Academy of Sciences, Kunming 650011, China

<sup>3</sup>University of the Chinese Academy of Science, Beijing 100049, China

<sup>4</sup>Department of Physics & Astronomy, University of Victoria, P.O. Box 3055, Victoria, B.C., V8W 3P6, Canada

<sup>5</sup>The Joint Institute for Nuclear Astrophysics, Notre Dame, IN 46556, USA

*Subject headings:* accretion, accretion disks — novae, cataclysmic variables — stars: evolution — supernovae: general — white dwarfs

## 1. Introduction

Type Ia supernovae (SNe Ia), as successful cosmological distance indicators, are thought to result from thermonuclear explosions of carbon-oxygen white dwarfs (CO WDs) in binaries. However, the nature of their progenitors still remains unclear. It is very likely that a CO WD grows somehow in mass close to the Chandrasekhar mass (Ch mass) of  $1.378 M_{\odot}$  (if its rotation is ignored) and then explodes as a SN Ia (e.g., Nomoto et al. 1984). The growth of a CO WD to the Ch mass limit has been investigated widely and many progenitor models of SNe Ia have been proposed in past years (for a detailed review, see Wang & Han 2012; Hillebrandt & Niemeyer 2000). The most popular progenitor models are single-degenerate (SD) and double-degenerate (DD) models. In the SD model, a CO WD accretes material from its non-degenerate companion to increase its mass close to the Ch mass (e.g., Whelan & Iben 1973; Nomoto et al. 1984; Han & Podsiadlowski 2004; Wang et al. 2009). In the DD model, two CO WDs spiral in due to gravitational wave radiation and eventually merge, leading to a SN Ia explosion (e.g., Iben & Tutukov 1984; Webbink 1984; Yungelson et al. 1994; Han 1998; Ruiter et al. 2009). The SD model has become the favourite one in the past decades because it can explain the similarities of SNe Ia and can reproduce very well characteristic observational features of most normal SNe Ia (see a recent review by Wang & Han 2012).

The process of accretion onto the CO WD is crucial for the SD scenario. At low accretion rates, the accreting WD undergoes H-shell flashes similar to nova outbursts (Gallagher & Starrfield 1978; Kovetz & Prialnik 1994; Prialnik & Kovetz 1995). However, multicycle evolution of the H-shell flash is difficult to compute, therefore only individual outbursts were followed in most simulations of novae. If the accretion rate is too high, the accreted matter will pile up on the surface of the WD and the WD will evolve into a star like a red giant (e.g., Nomoto 1982; Nomoto et al. 2007, hereafter NSKH07). Only in a narrow regime, is the H-shell burning steady, and the accreted hydrogen is burnt completely. The SN Ia birth rate based on this view was much lower than the observationally inferred one (e.g., Yungelson et al. 1996; Livio 2000). To solve this problem, the optically thick wind regime was proposed to replace the red giant regime (Kato & Hachisu 1994; Hachisu et al. 1996). In this regime, the H-rich matter is transformed into He at a critical rate,  $\dot{M}_{\text{cr}}$ , while the unprocessed material is

blown off by the optically thick wind. It significantly expanded the parameter space for the SN Ia progenitors, which resulted in a higher theoretical birth rate of SNe Ia from the SD scenario (Han & Podsiadlowski 2004; Meng et al. 2009). However, those studies did not pay much attention to the super-Eddington wind which is triggered when the luminosity of the accreting WD exceeds the Eddington luminosity. The Eddington accretion rate is around  $\sim 10^{-5} M_{\odot} \text{yr}^{-1}$  (Nomoto 1982; NSKH07), when only the accretion luminosity was used to evaluate the radiation pressure on the surface of the WD. Shen & Bildsten (2007) proposed that the nuclear burning (H-shell burning during accretion) near the surface of the WD has also to be considered when estimating the Eddington accretion rate. They obtained a range of Eddington accretion rate of  $2 - 7 \times 10^{-7} M_{\odot} \text{yr}^{-1}$  for various WD masses.

In this paper, we use the state-of-the-art stellar evolution code of MESA (version 3635) (Paxton et al. 2011, 2013) to simulate the long-term evolution of CO WDs accreting solar-composition material. Our aim is to investigate the stability of H-shell burning on these WDs. The WD masses range from 0.5 to  $1.378 M_{\odot}$ , while the accretion rate is varied from  $10^{-8}$  to  $10^{-5} M_{\odot} \text{yr}^{-1}$ . The Eddington accretion rate is estimated by including the nuclear energy, gravothermal energy and radiation of the core.

## 2. Simulation Code and Methods

In our study, we employed the MESA *default* opacity and EOS tables i.e. the same as described in Figures 1 and 2 in Paxton et al. (2011). Our nuclear network consisted of 21 isotopes, such as  $^1\text{H}$ ,  $^3\text{He}$ ,  $^4\text{He}$ ,  $^{12}\text{C}$ ,  $^{13}\text{C}$ ,  $^{13}\text{N}$ ,  $^{14}\text{N}$ ,  $^{15}\text{N}$ ,  $^{14}\text{O}$ ,  $^{15}\text{O}$ ,  $^{16}\text{O}$ ,  $^{17}\text{O}$ ,  $^{18}\text{O}$ ,  $^{17}\text{F}$ ,  $^{18}\text{F}$ ,  $^{19}\text{F}$ ,  $^{18}\text{Ne}$ ,  $^{19}\text{Ne}$ ,  $^{20}\text{Ne}$ ,  $^{22}\text{Mg}$ , and  $^{24}\text{Mg}$ , coupled by 50 reactions, including those of the pp chains and CNO cycles. Similar to NSKH07, the He-burning reactions were neglected for simplicity. Two relevant MESA suite cases were selected for simulations: `make_co_wd` and `wd2`.

The suite case `make_co_wd` was used to create CO WD models. First, we chose a sufficiently massive pre-MS star and evolved it until the mass of its He-exhausted core reached a value close to the final WD’s mass that we needed, but before its He shell began to experience thermal pulses. Then, we artificially removed the envelope, leaving a naked CO core that quickly evolved to the WD cooling track. We selected hot CO WD models on the

top of the cooling track as initial models for our accretion simulations<sup>1</sup>. Using these methods, we have obtained a series of CO WD models with masses in the range of  $0.5–1.0 M_{\odot}$ . For CO WDs with masses larger than  $1.0 M_{\odot}$ , we increased the mass of our naked  $1.0 M_{\odot}$  CO WD model by accreting material with its surface composition until the required mass was reached (Denissenkov et al. 2013). As a result, we created 12 CO WD models with the masses of 0.5, 0.6, 0.7, 0.8, 0.9, 1.0, 1.1, 1.2, 1.25, 1.3, 1.35 and  $1.378 M_{\odot}$ , with central temperatures of (in units of  $10^7\text{K}$ ) 7.5, 7.1, 7.0, 6.9, 7.7, 10.0, 10.4, 12.2, 13.7, 16.0, 20.7 and 25.2, respectively, at the onset of accretion.

The suite case of `wd2` was used to simulate accretion onto CO WDs. The accreted material has the solar composition, in particular, its H and heavy-element mass fractions are  $X = 0.7$  and  $Z = 0.02$ . We turned on a MESA option that allows to include the acceleration term in the equation of hydrostatic equilibrium. We have done a series of simulations for all of our CO WD models with the accretion rate in the range from  $10^{-8}$  to  $10^{-5} M_{\odot} \text{yr}^{-1}$ . Each simulation was carried out long enough to obtain its detailed accretion properties.

We realize that a real CO WD accretes material from its companion via an accretion disk. Therefore, the WD should initially accumulate the accreted material at its equator. However, this material will probably spread over the entire WD surface on a dynamical timescale because of a dynamical instability, resulting in its quasi-spherical distribution (MacDonald 1983). This motivates our assumption of spherically symmetric accretion, which is made and used for simplicity, like it was done previously in other similar studies (e.g. Iben & Tutukov 1989; Prialnik & Kovetz 1995; Hachisu et al. 1996, NSKH07, Shen & Bildsten 2007), although multi-dimensional simulations would provide more consistent results.

If the accretion rate is high enough, the luminosity  $L$  of the accreting WD may exceed the Eddington luminosity

$$L_{\text{Edd}} = \frac{4\pi GMc}{\kappa_T}, \quad (1)$$

where  $M$  is the WD mass and  $\kappa_T$  is the Thomson opacity<sup>2</sup>, in which case the super-Eddington wind is triggered.

---

<sup>1</sup>We encountered some convergence problems when simulating cold CO WDs, possibly due to the high degeneracy of materials on the surface of cold WDs and low resolution of WD models in our study (the total number of mass zones is typically around 2000). The evolution of cold CO WDs during accretion may be slightly different from that of the hot models before and at the onset of H burning, but the difference would become very small when an equilibrium state is achieved. Iben (1982) and Iben & Tutukov (1989) also used hot WD models when they simulated accreting WDs.

<sup>2</sup> We use the Thomson opacity here for comparison with previous work. However, in our calculation,  $\kappa_T$  was replaced by the opacity of the photosphere.

The total luminosity  $L$  consists of four parts, namely the nuclear burning energy, gravothermal energy released by compression, thermal radiation of the core, and accretion energy released by the accreted material. The nuclear burning luminosity,  $L_{\text{nuc}}$ , is always the main part of  $L$ . It can be written as

$$L_{\text{nuc}} = XQ\dot{M}_{\text{nuc}}, \quad (2)$$

where  $\dot{M}_{\text{nuc}}$ ,  $X$  and  $Q$  are the rate of the accretion material processed by hydrogen burning, hydrogen mass fraction in the accreted material, and the energy released per a unit mass of H transformed into He, respectively.

The accretion luminosity released by accreted material,  $L_{\text{acc}}$ , is

$$L_{\text{acc}} = \frac{GM\dot{M}_{\text{acc}}}{R}, \quad (3)$$

where  $M$  and  $R$  are WD's mass and radius, and  $\dot{M}_{\text{acc}}$  is the accretion rate.

By letting  $L_{\text{Edd}} = L_{\text{acc}}$ , the Eddington accretion rate is  $\dot{M}_{\text{Edd}} = 4\pi cR/\kappa_{\text{T}}$ , which was used in NSKH07. If  $L_{\text{Edd}} = L_{\text{nuc}}$  and  $\dot{M}_{\text{acc}} = \dot{M}_{\text{nuc}}$  (i.e. the accreted material is burnt completely), the Eddington accretion rate then becomes  $\dot{M}_{\text{Edd}} = 4\pi GMc/(\kappa_{\text{T}}XQ)$ , which was adopted in Shen & Bildsten (2007). Since  $L_{\text{nuc}} \gg L_{\text{acc}}$ , the value of  $\dot{M}_{\text{Edd}}$  obtained in Shen & Bildsten (2007) was much lower than that in NSKH07. Recently, Tauris et al. (2013) also obtained a much lower Eddington accretion limit than that of NSKH07 by setting  $L_{\text{Edd}} = L_{\text{nuc}} + L_{\text{acc}}$ .

Usually, the accretion energy is not taken into account in  $L$  because it is radiated away from the WD's surface very quickly (Townsend & Bildsten 2004). Here, we define a luminosity  $L_*$  as  $L - L_{\text{acc}}$  for convenience.

In our study, we first set  $L_{\text{Edd}} = L_{\text{acc}}$  as the wind triggering condition to reproduce the results of NSKH07 and examine the reliability of the method. Then, we let  $L_{\text{Edd}} = L_*$  as the wind triggering condition to study the behaviors of CO WDs during accretion, which is followed by a discussion of the inclusion of  $L_{\text{acc}}$  to  $L$ .

### 3. Results

#### 3.1. Reproducing Previous Results With the New Method

To directly compare with the results of the steady-state models of NSKH07, we first employed  $L_{\text{Edd}} = L_{\text{acc}}$  as the triggering condition for the super-Eddington wind. However,

the super-Eddington wind obtained under this condition cannot blow off a sufficient mass during an H-shell flash and, as a result, the calculation of the following evolution of the star is very CPU consumptive. Therefore, all simulations encountering H-shell flashes were investigated by setting  $L_{\text{Edd}} = L_*$ , while  $L_{\text{Edd}} = L_{\text{acc}}$  was set for other cases. Figure 1 shows three typical examples of our simulations: (a) an H-shell flash at a low accretion rate,  $10^{-7} M_{\odot} \text{yr}^{-1}$ ; (b) steady H burning at an intermediate accretion rate,  $2.1 \times 10^{-7} M_{\odot} \text{yr}^{-1}$ ; and (c) a WD becoming a red giant at a high accretion rate,  $8 \times 10^{-7} M_{\odot} \text{yr}^{-1}$  (hereafter, the red-giant regime). In panels (b) and (c), there are also weak H-shell flashes when H-rich material is ignited. Such an H-shell flash is unavoidable at any given accretion rate because H-rich material accumulated on the WD surface becomes electron-degenerate before it is initially ignited. Therefore, we first employed  $L_{\text{Edd}} = L_*$  as the triggering condition for the super-Eddington wind at the first H-shell flash, and only after that we set  $L_{\text{Edd}} = L_{\text{acc}}$  to simulate the following accretion evolution.

Figure 2 shows three boundary curves marked by their corresponding mass accretion rates:  $\dot{M}_{\text{stable}}$  separates the steady H burning from the H-shell flash,  $\dot{M}_{\text{RG}}$  separates the steady H burning from the red-giant regime, and  $\dot{M}_{\text{Edd}}$  separates the red-giant regime from the super-Eddington wind. All the boundaries were determined via bisection method for each WD mass. The results of Iben & Tutukov (1989) and NSKH07 are also presented in Figure 2 for comparison. It is seen that our results are very close to theirs. However, some differences exist in the exact locations of the boundary curves from our and previous works, which are likely caused by different methods employed. Iben & Tutukov (1989) used the static envelope analysis, NSKH07 used the linear stability analysis to investigate the stability of the steady-state models, while we carried out detailed stellar evolution calculations that included a realistic accretion process. A detailed comparison of parameters of the WD models in the steady H burning regimes obtained in our work and in NSKH07 is made in Table 1. Again, we see that the two models have very similar properties.

### 3.2. The Super-Eddington Wind Scenario

Here, we employ  $L_{\text{Edd}} = L_*$  as a condition for triggering the super-Eddington wind to calculate the Eddington accretion rate ( $\dot{M}_{\text{Edd}}$ ) for each WD mass. The results are shown in Figure 3. We find that the values of  $\dot{M}_{\text{Edd}}$  in this case are much lower than those from the previous works, even lower than the values of  $\dot{M}_{\text{RG}}$  obtained in section 3.1. The entire red-giant regime is now replaced by a new regime that we call the “super-Eddington wind regime”. In this new regime, material accreted onto the surface of the WD first undergoes an

H-shell flash. After that, the H burning becomes steady and then the super-Eddington wind is triggered. The super-Eddington wind continues to blow off the surface material, which prevents the envelope from expanding, then the WD will never become a red giant and its luminosity remains constant at a value of the Eddington luminosity.

In the super-Eddington wind regime, H burning is stable, and the accreted material is partially accumulated on the WD surface. Furthermore, the WD mass growth rate equals approximately to  $\dot{M}_{\text{Edd}}$ . The extra mass is blown away by the super-Eddington wind. Thus, the super-Eddington wind is an alternative to the optically thick wind in preventing an accreting WD from expanding to a red giant at relatively high accretion rates. For a convenient use, we have fitted our  $\dot{M}_{\text{Edd}}$  and  $\dot{M}_{\text{stable}}$  data by the following polynomials:

$$\dot{M}_{\text{Edd}} = 5.975 \times 10^{-6} (M_{\text{WD}}^4 - 3.496M_{\text{WD}}^3 + 4.373M_{\text{WD}}^2 - 2.226M_{\text{WD}} + 0.406), \quad (4)$$

$$\dot{M}_{\text{stable}} = 3.057 \times 10^{-7} (M_{\text{WD}}^2 - 0.386M_{\text{WD}} + 0.027), \quad (5)$$

where  $M_{\text{WD}}$  is in units of  $M_{\odot}$ , and  $\dot{M}_{\text{Edd}}$  and  $\dot{M}_{\text{stable}}$  are both in units of  $M_{\odot} \text{ yr}^{-1}$ .

In the above analysis, we neglected a contribution of  $L_{\text{acc}}$  to  $L$ . However, for massive WDs, say  $1.35M_{\odot}$ ,  $L_{\text{acc}} \sim 10^3L_{\odot}$  and it contributes to  $L$  as much as 10 per cent (Frank et al. 1985). The inclusion of  $L_{\text{acc}}$  in  $L$  will make the super-Eddington wind to occur more easily, because an additional source of energy will be contributing to expelling the accreted material. Given that part of the accretion luminosity is emitted by the disk, and a part of the rest of it goes into spinning up of the WD (Lynden-Bell & Pringle 1974; Balsara et al. 2009)<sup>3</sup>, we examined the effect of  $L_{\text{acc}}$  for the following three cases:  $L_{\text{Edd}} = L_* + 0.1L_{\text{acc}}$ ,  $L_{\text{Edd}} = L_* + 0.5L_{\text{acc}}$ , and  $L_{\text{Edd}} = L_* + 0.8L_{\text{acc}}$ . The corresponding results are also shown in Figure 3, in which we see that the Eddington accretion limit *does* decrease with the inclusion of  $L_{\text{acc}}$  for massive CO WDs, while little differences exist in low-mass WDs.

#### 4. Discussion and Conclusion

We have investigated the evolution of accreting CO WDs with masses from 0.5 to  $1.378M_{\odot}$  for accretion rates from  $10^{-8}$  to  $10^{-5}M_{\odot} \text{ yr}^{-1}$ . Our results are consistent with those from the previous studies of the properties of H burning on the surfaces of CO WDs during accretion, except for some differences in the exact locations of the boundaries between

---

<sup>3</sup>The energy deposited to winds is usually less than  $0.5L_{\text{acc}}$ .

different regimes. We have proposed the super-Eddington wind regime to replace the optical thick wind regime in preventing the WD’s envelope from expanding at high accretion rates. If a CO WD accretes material with an appropriate rate (i.e. above  $\dot{M}_{\text{Edd}}$ ), the WD will evolve through the super-Eddington wind regime. The H in the accreted material is burnt into He at a rate around  $\dot{M}_{\text{Edd}}$  and the unprocessed material is blown away by the super-Eddington wind. If the underlying He is further burnt into C and O as assumed in the literature, the WD mass then increases and possibly reaches the Ch mass. This picture thus provides a potential scenario for the progenitors of SNe Ia. Note that we assumed a constant accretion rate in our study, but the strong winds may hit the companion surface and should affect the mass transfer rate to such an extent that it could eventually stop (Hachisu et al. 1999).

The characteristics of the super-Eddington wind are similar to those of the optically thick wind (Hachisu et al. 1996). However, the efficiency of the optically thick wind strongly depends on the metallicity because it is driven by a peak in the opacity due to iron lines, therefore it does not work when the metallicity is lower than 0.002 (Kobayashi et al. 1998; Kobayashi & Nomoto 2009). On the contrary, the super-Eddington wind does not significantly depend on the metallicity. We examined this for two CO WDs (with mass of 1.0 and  $1.378M_{\odot}$ , respectively) for  $Z = 10^{-6}$ , and found that the super-Eddington wind could still be triggered. The extra mass exceeding the Eddington accretion rate is blown away by the super-Eddington wind, and the WDs increase in mass with rates near the Eddington accretion rate (see Figure 4). This indicates that our super-Eddington wind scenario may produce SNe Ia at very low metallicities, which could explain the SNe Ia at high redshifts, e.g. SN UDS10Wil with a redshift of 1.914 (Jones et al 2013), assuming that the metallicity decreases with the redshift.

Note that the mass-loss rate ( $\equiv \dot{M}_{\text{acc}} - \dot{M}_{\text{Edd}}$  in our study) by super-Eddington wind has an upper limit,  $\dot{M}_{\text{max}}$ , above which the super-Eddington wind cannot blow away all the unprocessed material. From the energy limit (Langer et al. 2000),  $\dot{M}_{\text{max}} = (\alpha L/L_{\text{Edd}}) 6 \times 10^{-6} (R/0.01R_{\odot}) M_{\odot} \text{yr}^{-1}$ , where  $L$  is the star luminosity and  $\alpha$  is the efficiency of stellar photon luminosity converting into kinetic wind energy ( $\alpha = 1$  if we assume all the photon energy is used to drive the wind i.e all photons have been trapped and the WD is invisible). If  $\dot{M}_{\text{acc}} > \dot{M}_{\text{Edd}} + \dot{M}_{\text{max}}$ , the WD may then become a red giant eventually.<sup>4</sup>

We have not considered abundance mixing induced by H-shell flashes in our study, since the underlying He shell grows in each H-shell flash and prevents any dredge-up of heavier nuclei from the core to the surface zone (Kovetz & Prialnik 1994). The abundance mixing

---

<sup>4</sup>The mass-loss rate of optically thick wind (Hachisu et al. 1996) is also limited by the energy limit. For Wolf-Rayet stars,  $\alpha \simeq 0.05$  from the study of Lucy & Abbott (1993).

might affect the energy production via nuclear burning, and then the  $\dot{M}_{\text{stable}}$  boundary slightly, but not the super-Eddington wind boundary.

We acknowledge useful discussions and suggestions from Xiangdong Li. This work is partly supported by the NSFC (Nos.11173055, 11033008) and Yunnan Grant (2012HB037). PAD acknowledges the support of his research by the NSF grants PHY 11-25915 and AST 11-09174 and by JINA (NSF grant PHY 08-22648). The computations are made at the Yunnan Observatories Supercomputing Platform.

## REFERENCES

- Balsara, D. S., Fisker, J. L., Godon, P., Sion, E. M. 2009, *ApJ*, 702, 1536
- Denissenkov, P. A., Herwig, F., Bildsten, L., Paxton, B. 2013, *ApJ*, 762, 8D
- Frank, J., King, A. R., & Raine, D. J. 1985, *Accretion Power in Astrophysics* (Cambridge: Cambridge Univ. Press), 283 p
- Gallagher, J. S., & Starrfield, S. 1978, *ARA&A*, 16, 171
- Han, Z. 1998, *MNRAS*, 296, 1019
- Han, Z., Podsiadlowski, Ph. 2004, *MNRAS*, 350, 1301
- Hachisu, I., Kato, M., Nomoto, K. 1996, *ApJ*, 470, L97
- Hachisu, I., Kato, M., Nomoto, K. 1999, *ApJ*, 522, 487
- Hillebrandt, W., & Niemeyer, J. 2000, *ARA&A*, 38, 191
- Iben, I., Jr., 1982, *ApJ*, 259, 244
- Iben, I., Jr., & Tutukov, A. V. 1984, *ApJS*, 54, 335
- Iben, I., Jr., & Tutukov, A. V. 1989, *ApJ*, 342, 430
- Jones, D. O., Rodney, S. A., Riess, A. G. et al 2013, *ApJ*, 768, 166
- Kato, M., Hachisu, I. 1994, *ApJ*, 437, 802
- Kobayashi, C., & Nomoto, K. 2009, *ApJ*, 707, 1466
- Kobayashi, C., Tsujimoto, T., Nomoto, K., Hachisu, I., Kato, M. 1998, *ApJ*, 503, L155

- Kovetz, A., & Prialnik, D. 1994, *ApJ*, 424, 319
- Langer, N., Deutschmann, A., Wellstein, S., Hflich, P. 2000, *ApJ*, 362, 1046
- Livio, M. 2000, in *Type Ia Supernovae: Theory and Cosmology*, eds. J. C. Niemeyer & J. W. Truran (Cambridge: Cambridge Univ. Press), 33
- Lucy, L. B., Abbott, D. C. 1993, *ApJ*, 405, 738
- Lynden-Bell, D., & Pringle, J. E. 1974, *MNRAS*, 168, 303
- MacDonald, J. 1983, *ApJ*, 273, 289
- Meng, X., Chen, X., Han, Z. 2009, *MNRAS*, 395, 2103
- Nomoto, K. 1982, *ApJ*, 253, 798
- Nomoto, K., Thielemann, F., Yokoi, K. 1984, *ApJ*, 286, 644
- Nomoto, K., Saio, H., Kato, M., Hachisu, I. 2007, *ApJ*, 663, 1269 (NSKH07)
- Paxton, B., Bildsten, L., Dotter, A., Herwig, F., Lessafre, P., Timmes, F. 2011, *ApJS*, 192, 3
- Paxton, B., Cantiello, M., Arras, Ph., Bildsten, L., Brown, E., Dotter, A., Mankovich, C., Montgomery, M. H., Stello, D., Timmes, F. X., Townsend, R. 2013, *ApJS*, 208, 4
- Prialnik, D., & Kovetz, A. 1995, *ApJ*, 445, 789
- Ruiter, A. J., Belczynski, K., Fryer, C. 2009, *ApJ*, 699, 2026
- Shen, K. J., & Bildsten, L. 2007, *ApJ*, 660, 1444
- Tauris, T. M., Sanyal, D., Yoon, S. -C., Langer, N. 2013, *astro-ph*, 1308.4887
- Townsley, D. M., & Bildsten, L. 2004, *ApJ*, 600, 390
- Wang, B., Chen, X., Meng, X., Han, Z. 2009, *ApJ*, 701, 1540
- Wang, B., & Han, Z. 2012, *NewAR*, 56, 122
- Webbink, R. F. 1984, *ApJ*, 277, 355
- Whelan, J., & Iben, I., Jr. 1973, *ApJ*, 186, 1007
- Yungelson, L. R., Livio, M., Tutukov, A. V., Saffer, R. A. 1994, *ApJ*, 420, 336

Yungelson, L., Livio, M., Truran, J. W., Tutukov, A., Fedorova, A. 1996 ApJ 466, 890

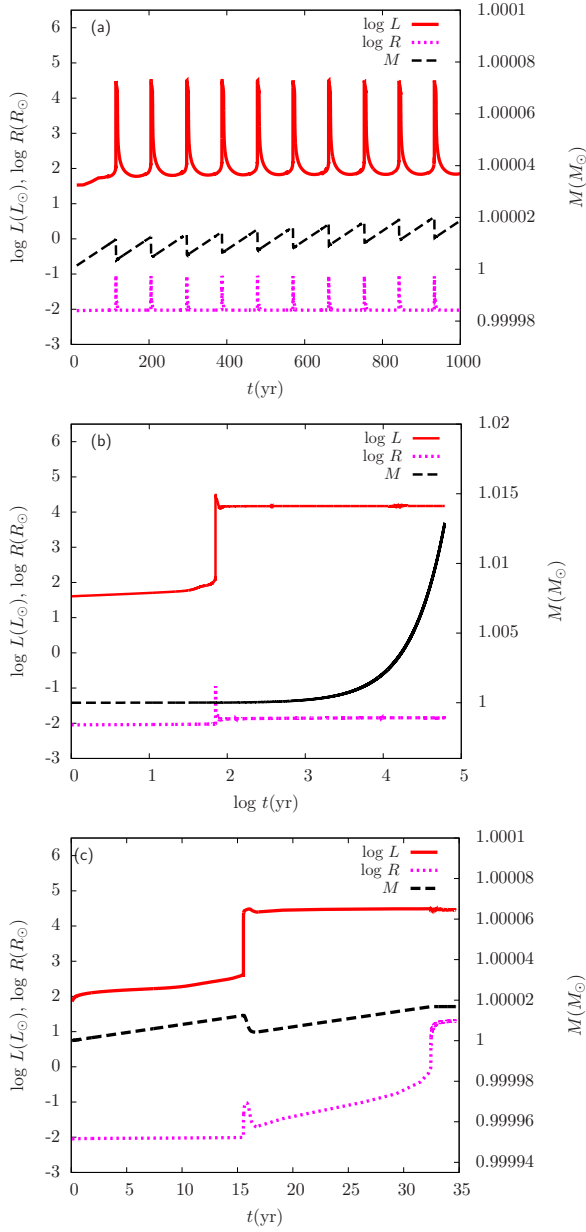


Fig. 1.— Temporal evolution of the luminosity, radius, and mass of an accreting  $1 M_\odot$  CO WD in the H-shell flash case ( $\dot{M}_{\text{acc}} \sim 10^{-7} M_\odot \text{ yr}^{-1}$ , panel a), in the steady H burning case ( $\dot{M}_{\text{acc}} \sim 2.1 \times 10^{-7} M_\odot \text{ yr}^{-1}$ , panel b), and in the red-giant regime ( $\dot{M}_{\text{acc}} \sim 8 \times 10^{-7} M_\odot \text{ yr}^{-1}$ , panel c).

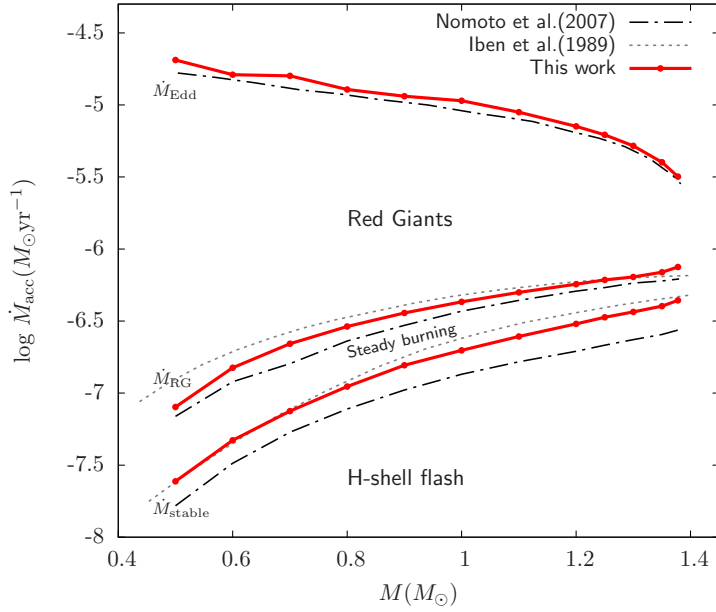


Fig. 2.— Properties of H burning on the surfaces of accreting CO WDs in the WD mass-accretion rate plane. The super-Eddington wind is triggered when  $L_{\text{acc}} = L_{\text{Edd}}$ . The red solid curves are the results of our calculations. The black dot-dashed curves and the grey dotted curves are from NSKH07 and Iben & Tutukov (1989), respectively. Note that Iben & Tutukov (1989) did not present their  $\dot{M}_{\text{Edd}}$  in their paper.

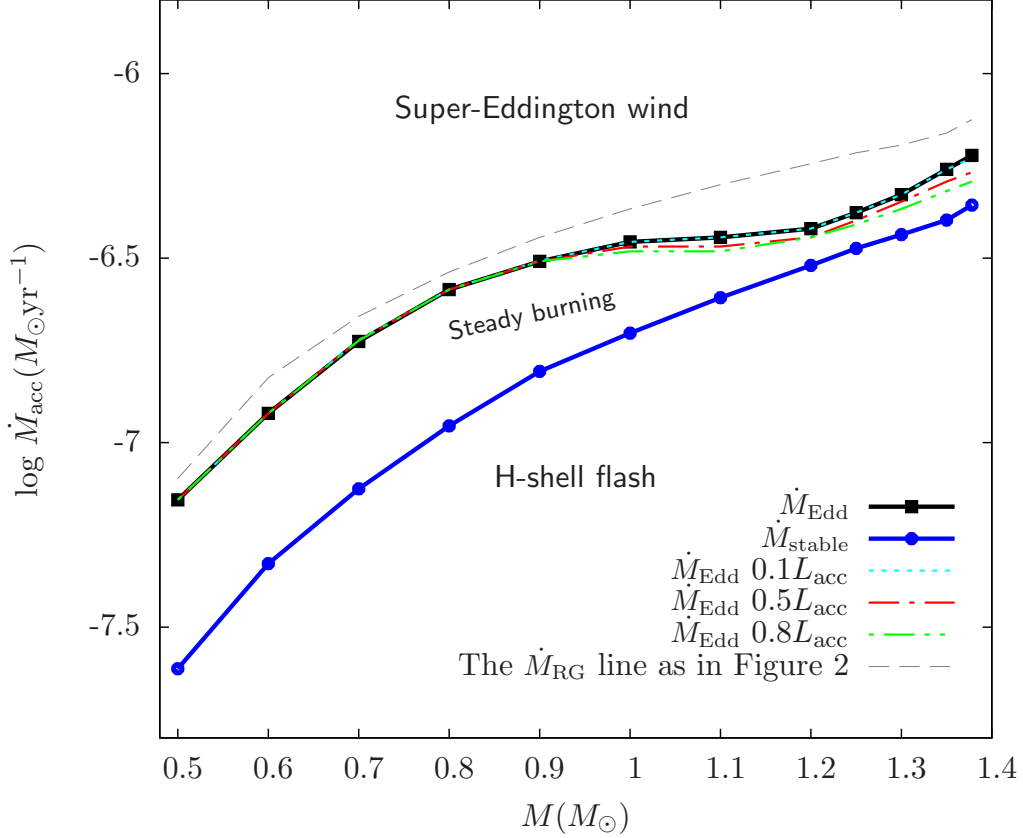


Fig. 3.— Similar to Figure 2, but the super-Eddington wind is triggered when  $L_* = L_{\text{Edd}}$  (the thick solid curves). The light blue dotted, red dot-dashed and green dash-dot-dotted lines show the Eddington accretion limits by adopting  $L_{\text{Edd}} = L_* + 0.1L_{\text{acc}}$ ,  $L_{\text{Edd}} = L_* + 0.5L_{\text{acc}}$  and  $L_{\text{Edd}} = L_* + 0.8L_{\text{acc}}$ , respectively. The super-Eddington wind starts much earlier and the boundary of  $\dot{M}_{\text{RG}}$  does not exist in this condition. For a comparison, the grey dashed curve shows the boundary of  $\dot{M}_{\text{RG}}$  presented in Figure 2.

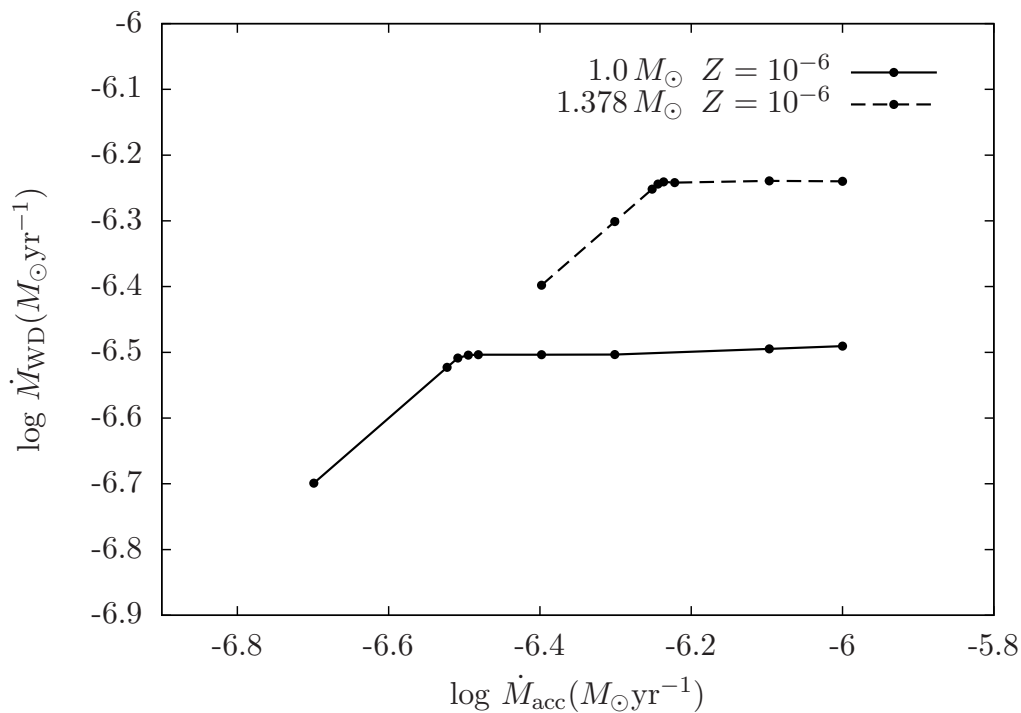


Fig. 4.— The CO WD mass growth rate,  $\dot{M}_{\text{WD}}$ , versus accretion rate at a metallicity  $10^{-6}$ . The Eddington accretion rate is  $3.1 \times 10^{-7} M_{\odot} \text{yr}^{-1}$  for a  $1 M_{\odot}$  CO WD, and  $5.7 \times 10^{-7} M_{\odot} \text{yr}^{-1}$  for a  $1.378 M_{\odot}$  CO WD. If the accretion rate is higher than the Eddington accretion rate, the extra mass is blown away by the super-Eddington wind and the mass growth rate of the WD approximately equals to the Eddington accretion rate.

Table 1. Characteristics of two WD models during steady H burning

Property	NSKH07	This work	NSKH07	This work
$M_{\text{WD}}(M_{\odot})$	0.8	0.8	1.0	1.0
$\Delta M_{\text{env}}(M_{\odot})$	$2.0 \times 10^{-5}$	$2.0 \times 10^{-5}$	$3.9 \times 10^{-6}$	$6.8 \times 10^{-6}$
$\dot{M}_{\text{acc}}(M_{\odot}\text{yr}^{-1})$	$2.2 \times 10^{-7}$	$2.2 \times 10^{-7}$	$2.5 \times 10^{-7}$	$2.5 \times 10^{-7}$
$\log r_{\text{H}}(R_{\odot})$	-1.888	-1.905	-2.034	-2.029
$\log T_{\text{H}}(\text{K})$	7.89	7.85	7.93	7.88
$\log \rho_{\text{H}}(\text{g cm}^{-3})$	1.01	1.01	1.20	1.20
$\log P_{\text{H}}(\text{dyn cm}^{-2})$	17.31	17.17	17.50	17.34
$\log L_{\text{nuc}}(L_{\odot})$	4.188	4.177	4.243	4.245
$\log L(L_{\odot})$	4.218	4.185	4.274	4.256
$\log R(R_{\odot})$	-1.255	-1.515	-1.792	-1.834
$\log T_{\text{eff}}(\text{K})$	5.444	5.565	5.726	5.743

Note. —  $M_{\text{WD}}$  is the WD mass,  $\dot{M}_{\text{acc}}$  is the accretion rate, and  $\Delta M_{\text{env}}$  is the mass of the H-rich envelope.  $r_{\text{H}}$ ,  $T_{\text{H}}$ ,  $\rho_{\text{H}}$  and  $P_{\text{H}}$  are the radius, temperature, density and pressure, respectively, at the bottom of the H-rich envelope.  $L$ ,  $L_{\text{nuc}}$ ,  $R$  and  $T_{\text{eff}}$  are the luminosity, nuclear burning luminosity, radius and effective temperature, respectively, at the surface.